

# A Comparison of the Extended and Unscented Kalman Filters for Discrete-Time Systems with Nondifferentiable Dynamics

J. Chandrasekar, A. J. Ridley, and D. S. Bernstein

**Abstract**—We compare the performance of the extended Kalman filter, the unscented Kalman filter, and two extensions of the  $H_\infty$  filter when applied to discrete-time nonlinear state estimation problems with nondifferentiable dynamics. We compare the performance of all the estimation techniques on simple nonlinear examples and finally consider state estimation of one-dimensional hydrodynamic flow based on a finite volume model that contains nondifferentiable nonlinearities.

## I. INTRODUCTION

Because of the widespread need for nonlinear observers and estimators, this area of research remains one of the most active [1, 2]. One of the main drivers of research in this area is applications to distributed, large scale systems, the most visible of which is weather forecasting [3]. This area is often referred to as data assimilation.

The classical Kalman filter for linear systems is often applied to nonlinear systems in the form of the extended Kalman filter (XKF) [4, 5]. A variation of XKF is the state-dependent Riccati equation (SDRE) approach, in which, in place of the Jacobians, the dynamics and output map are exactly factored, and the factors are used for the pseudo-covariance update [6, 7].

Another approach to state estimation of linear systems are the  $H_\infty$  filters [8]. Unlike the classical Kalman filter, these filters do not require the stringent Gaussian distribution assumption on the process and sensor noise affecting the system, and guarantee a performance bound. Estimation with uncertainty in the model has also been performed using the  $H_\infty$  filter [9]. We apply the  $H_\infty$  filter to nonlinear systems by using the Jacobians of the dynamics and measurement maps and call the resulting filter the extended  $H_\infty$  filter (XHF).

Yet another approach to nonlinear estimation involves particle filters. Among the various techniques that have been developed are the unscented Kalman filter (UKF) [10, 11], which deterministically constructs the collection of state estimates. Although particle filters do not require the propagation of a covariance (or pseudo-covariance) in the usual (Riccati) way, the size of the collection determines the computational requirements. Finally, we combine the  $H_\infty$  filter gain expression with the particle filter framework to obtain the unscented  $H_\infty$  filter (UHF).

The present paper focuses on discrete-time systems with dynamics that are not differentiable. The main motivation is state estimation based on computational fluid dynamics

(CFD) models for space weather forecasting [12]. In particular we focus on CFD models for hydrodynamics (HD) and magnetohydrodynamics (MHD) in which the equations of fluid motion are approximated by finite volume schemes. In [6] we have considered SDRE and XKF methods for state estimation of one-dimensional hydrodynamic flow.

In HD and MHD, the CFD models involve nondifferentiable functions as part of the discretization of the underlying partial differential equations [13]. In the present paper, we consider an alternative approach in which we apply XKF and XHF despite the lack of differentiability. In particular, we compute the Jacobian at all points at which it exists, and we employ an averaged value at points at which the dynamics are not differentiable. To demonstrate the accuracy of XKF, XHF, UKF, and UHF when the dynamics are not differentiable, we consider several examples. We are interested in both the accuracy and computational requirements of each approach.

## II. THE KALMAN FILTER

Consider the discrete-time linear system with dynamics

$$x_{k+1} = A_k x_k + B_k u_k + w_k \quad (2.1)$$

and measurements

$$y_k = C_k x_k + v_k, \quad (2.2)$$

where  $x_k \in \mathbb{R}^n$ ,  $u_k \in \mathbb{R}^m$ , and  $y_k \in \mathbb{R}^p$ . The input  $u_k$  and output  $y_k$  is assumed to be measured, and  $w_k \in \mathbb{R}^n$  and  $v_k \in \mathbb{R}^p$  are uncorrelated zero-mean white noise processes with covariances  $Q_k$  and  $R_k$ , respectively. We assume that  $R_k$  is positive definite.

For the system (2.1) and (2.2), the Kalman filter provides optimal estimates of the state  $x_k$  using measurements  $y_k$  [14]. The Kalman filter equations can be expressed in two steps, namely, the data assimilation step

$$K_k = P_k^f C_k^T (R_k^f)^{-1}, \quad (2.3)$$

$$P_k^{da} = P_k^f - P_k^f C_k^T (R_k^f)^{-1} C_k P_k^f, \quad (2.4)$$

$$x_k^{da} = x_k^f + K_k (y_k - y_k^f), \quad (\text{data update}) \quad (2.5)$$

$$y_k^f = C_k x_k^f, \quad (2.6)$$

where  $R_k^f \triangleq C_k P_k^f C_k^T + R_k$ , and the forecast step

$$x_{k+1}^f = A_k x_k^{da} + B_k u_k, \quad (\text{physics update}) \quad (2.7)$$

$$P_{k+1}^f = A_k P_k^{da} A_k^T + Q_k, \quad (2.8)$$

where the *data assimilation error covariance*  $P_k^{da} \in \mathbb{R}^{n \times n}$  and the *forecast error covariance*  $P_k^f \in \mathbb{R}^{n \times n}$  are defined

This research was supported by the National Science Foundation, through Grant ATM-0325332 to the University of Michigan, Ann Arbor, USA. The authors are with the University of Michigan, Ann Arbor, MI-48109, dsbaero@umich.edu.

by  $P_k^f \triangleq \mathcal{E} [e_k^f (e_k^f)^T]$ ,  $P_k^{\text{da}} \triangleq \mathcal{E} [e_k^{\text{da}} (e_k^{\text{da}})^T]$ , and the *data assimilation error state*  $e_k^{\text{da}}$  and *forecast error state*  $e_k^f$  are defined by  $e_k^{\text{da}} \triangleq x_k - x_k^{\text{da}}$ ,  $e_k^f \triangleq x_k - x_k^f$ . Note that the Kalman filter gain  $K_k$  in (2.3) minimizes the cost function  $J_k(K_k) = \text{tr}(P_{k+1}^f)$ .

### III. THE $H_\infty$ FILTER

Consider the cost function

$$J(K_k) = \frac{\sum_{i=0}^N (e_i^f)^T M e_i^f}{(e_0^f)^T P_0^f e_0^f + \sum_{i=0}^N w_i^T Q w_i + \sum_{i=0}^N v_i^T R v_i}. \quad (3.1)$$

The  $H_\infty$  filter ensures that inspite of the worst possible process and sensor noise, the cost  $J(K_k)$  satisfies

$$J(K_k) \leq \frac{1}{\gamma}. \quad (3.2)$$

The data assimilation step of the robust  $H_\infty$  filter is given by

$$x_k^{\text{da}} = x_k^f + K_k(y_k - y_k^f), \quad (3.3)$$

$$y_k^f = C x_k^f, \quad (3.4)$$

$$P_k^{\text{da}} = (I - K_k C) \tilde{P}_k^f (I - K_k C)^T + K_k R K_k^T, \quad (3.5)$$

where

$$K_k = \tilde{P}_k^f C^T (C \tilde{P}_k^f C^T + R)^{-1} \quad (3.6)$$

and

$$\tilde{P}_k^f \triangleq P_k^f (I - \gamma M P_k^f)^{-1}. \quad (3.7)$$

The forecast step of the  $H_\infty$  filter is given by

$$x_{k+1}^f = A_k x_k^{\text{da}}, \quad (3.8)$$

$$P_{k+1}^f = A_k P_k^{\text{da}} A_k^T + Q. \quad (3.9)$$

Note that unlike the Kalman filter,  $w_k$  and  $v_k$  need not be white noise processes and hence  $Q$  and  $R$  are not their covariances, but a weighting on the uncertainty associated with the process and sensor noise. Moreover,  $P_k^f$  and  $P_k^{\text{da}}$  in (3.3)-(3.9) are not the error covariances.

### IV. THE EXTENDED KALMAN FILTER

Next, we consider the discrete-time nonlinear system with dynamics

$$x_{k+1} = f(x_k, u_k, k) + w_k \quad (4.1)$$

and measurements

$$y_k = h(x_k, k) + v_k. \quad (4.2)$$

The two-step XKF is given by

$$x_{k+1}^f = f(x_k^{\text{da}}, u_k, k), \quad (4.3)$$

$$x_k^{\text{da}} = x_k^f + K_k(y_k - y_k^f), \quad (4.4)$$

$$y_k^f = h(x_k^f, k), \quad (4.5)$$

where  $K_k$ ,  $P_k^{\text{da}}$  and  $P_k^f$  are given by (2.3), (2.4) and (2.8), respectively, with

$$A_k \triangleq \left. \frac{\partial f(x, u, k)}{\partial x} \right|_{x=x_k^{\text{da}}, u=u_k}, \quad C_k \triangleq \left. \frac{\partial h(x, k)}{\partial x} \right|_{x=x_k^{\text{da}}}. \quad (4.6)$$

If  $f(x, u, k)$  and  $h(x, k)$  are not differentiable with respect to  $x$ , XKF in (4.3)-(4.6) cannot be used because  $A_k$  and  $C_k$  defined in (4.6) may not exist for all  $x_k^{\text{da}}$ . However, we assume that the first order symmetric partial derivatives [16] of  $f(x, u, k)$  and  $h(x, k)$  exist everywhere, that is, for all  $x \in \mathbb{R}^n$ ,

$$\left. \frac{\partial_s f(\xi, u, k)}{\partial_s \xi_i} \right|_{\xi=x} \triangleq \lim_{\delta \rightarrow 0} \frac{f(x + \delta e_i, u, k) - f(x - \delta e_i, u, k)}{2\delta} \quad (4.7)$$

and

$$\left. \frac{\partial_s h(\xi, k)}{\partial_s \xi_i} \right|_{\xi=x} \triangleq \lim_{\delta \rightarrow 0} \frac{h(x + \delta e_i, k) - h(x - \delta e_i, k)}{2\delta} \quad (4.8)$$

exist, where  $\xi \in \mathbb{R}^n$  has scalar entries  $\xi = [\xi_1 \ \cdots \ \xi_n]^T$  and  $e_i \in \mathbb{R}^n$  is the  $i$ th column of the  $n \times n$  identity matrix. Hence, for example, although  $f(x) = |x|$  does not have a derivative at  $x = 0$ , it follows from (4.7) that  $\left. \frac{\partial_s f}{\partial_s x} \right|_{x=0} = 0$ . Furthermore, if  $g: \mathbb{R}^n \rightarrow \mathbb{R}$  is a differentiable function, then the symmetric partial derivative and the partial derivative are equal.

Next, we define the  $(i, j)$  entry of the averaged Jacobian  $F_s(x, u, k) \in \mathbb{R}^{n \times n}$  and  $H_s(x, k) \in \mathbb{R}^{p \times n}$  of  $f(\cdot)$  and  $h(\cdot)$ , respectively, by

$$F_{s,i,j}(x, u, k) \triangleq \left. \frac{\partial_s f_i(\xi, u, k)}{\partial_s \xi_j} \right|_{\xi=x}, \quad H_{s,i,j}(x, k) \triangleq \left. \frac{\partial_s h_i(\xi, k)}{\partial_s \xi_j} \right|_{\xi=x}, \quad (4.9)$$

where  $f_i(x, u, k)$  and  $h_i(x, k)$  are the scalar entries of  $f(x, u, k) \in \mathbb{R}^n$  and  $h(x, k) \in \mathbb{R}^p$ , respectively. Note that if  $f(\cdot)$  and  $h(\cdot)$  are differentiable, then, for all  $x \in \mathbb{R}^n$ , the averaged Jacobians  $F_s$  and  $H_s$  are equal to the true Jacobians. Hence, XKF for (4.1)-(4.2) when  $f(\cdot)$  and  $h(\cdot)$  satisfy (4.7) and (4.8) is given by (4.3), where  $K_k$ ,  $P_k^{\text{da}}$  and  $P_k^f$  are given by (2.3), (2.4) and (2.8), respectively, with

$$A_k = F_s(x_k^{\text{da}}, u_k, k), \quad C_k = H_s(x_k^{\text{da}}, k). \quad (4.10)$$

### V. THE EXTENDED $H_\infty$ FILTER

An alternative approach to state estimation of (4.1)-(4.2) is based on the  $H_\infty$  filter. Although, the  $H_\infty$  filter is derived for linear time-invariant systems, like the extended Kalman filter, the Jacobian of the dynamics and measurements maps can be used in the filter equations. However, the performance bounds guaranteed in the linear case are not valid anymore.

The extended  $H_\infty$  filter (XHF) is given by (4.3)-(4.5), where  $K_k$ ,  $P_k^{\text{da}}$  and  $P_k^f$  are given by (3.5)-(3.7) and (3.9), with  $A_k$  and  $C_k$  defined by (4.10). Note that since the Jacobians are based on the symmetric derivatives, XHF that uses the averaged Jacobians can be used on nonlinear systems with nondifferentiable dynamics. Finally, we use  $\gamma$ ,  $Q$  and  $R$  in XHF as tuning parameters to improve the estimates. Note that XHF may not be stable for all values of  $\gamma$  and hence  $\gamma$  must be tuned carefully.

### VI. THE UNSCENTED KALMAN FILTER

Another approach to state estimation of nonlinear systems is the unscented Kalman filter (UKF). The starting point for UKF is a set of sample points, that is, a collection of state estimates that capture the initial probability distribution of the state [10].

Assume that  $\bar{x} \in \mathbb{R}^n$ ,  $\bar{P} \in \mathbb{R}^{n \times n}$  is positive semidefinite and  $\lambda > 0$ . The unscented transformation is used to obtain  $2n + 1$  sample points  $X_i \in \mathbb{R}^n$  and corresponding weights  $\gamma_{x,i}$  and  $\gamma_{P,i}$ , for  $i = 0, \dots, 2n$ , so that the weighted mean and the weighted variance of the sample points is  $\bar{x}$  and  $\bar{P}$ , respectively. The unscented transformation  $X = \Psi(\bar{x}, \bar{P}, \lambda)$  of  $\bar{x}$  with covariance  $\bar{P}$  is defined by

$$X_i = \begin{cases} \bar{x}, & \text{if } i = 0, \\ \bar{x} + \tilde{P}_i, & \text{if } i = 1, \dots, n, \\ \bar{x} - \tilde{P}_{i-n}, & \text{if } i = n + 1, \dots, 2n, \end{cases} \quad (6.1)$$

where  $\tilde{P} \triangleq (\lambda \bar{P})^{1/2}$ , for  $i = 1, \dots, n$ ,  $\tilde{P}_i$  is the  $i$ th column of  $\tilde{P}$ ,  $X \in \mathbb{R}^{n \times 2n+1}$  has entries  $X = [X_0 \ \dots \ X_{2n}]$  and  $\lambda$  determines the spread of the sample points around  $\bar{x}$ . Note that  $\sum_{i=0}^{2n} \gamma_{x,i} X_i = \bar{x}$ , and  $\sum_{i=0}^{2n} \gamma_{P,i} (X_i - \bar{x})(X_i - \bar{x})^T = \bar{P}$ , where the weights are defined by  $\gamma_{x,0} \triangleq \frac{\lambda-n}{\lambda}$ ,  $\gamma_{P,0} \triangleq \frac{\lambda-n}{\lambda} + (1 - \frac{\lambda}{n} + \beta)$ , where  $\beta > 0$ , and for  $i = 1, \dots, 2n$ ,  $\gamma_{x,i} = \gamma_{P,i} \triangleq \frac{1}{2\lambda}$ .

The analysis step of the unscented Kalman filter is given by

$$x_k^{\text{da}} = x_k^{\text{f}} + K_k(y_k - y_k^{\text{f}}), \quad (6.2)$$

$$y_k^{\text{f}} = h(x_k^{\text{f}}, k), \quad (6.3)$$

$$X_k^{\text{da}} = \Psi(x_k^{\text{da}}, P_k^{\text{da}}, \lambda), \quad (6.4)$$

$$P_k^{\text{da}} = P_k^{\text{f}} - K_k P_{yy,k} K_k^T, \quad (6.5)$$

where

$$K_k = P_{xy,k} P_{yy,k}^{-1}, \quad (6.6)$$

$$P_{xy,k} = \sum_{i=0}^{2n} \gamma_{P,i} (X_{i,k}^{\text{f}} - x_k^{\text{f}})(Y_{i,k}^{\text{f}} - y_k^{\text{f}})^T, \quad (6.7)$$

$$P_{yy,k} = \sum_{i=0}^{2n} \gamma_{P,i} (Y_{i,k}^{\text{f}} - y_k^{\text{f}})(Y_{i,k}^{\text{f}} - y_k^{\text{f}})^T + R_k, \quad (6.8)$$

$$Y_{i,k}^{\text{f}} = h(X_{i,k}^{\text{f}}, k), \quad (6.9)$$

and the forecast step of the unscented Kalman filter is given by

$$\hat{X}_{i,k+1}^{\text{f}} = f(X_{i,k}^{\text{da}}, k), \quad (6.10)$$

$$x_{k+1}^{\text{f}} = \sum_{i=0}^{2n} \gamma_{x,i} \hat{X}_{i,k+1}^{\text{f}}, \quad (6.11)$$

$$P_{k+1}^{\text{f}} = \sum_{i=0}^{2n} \gamma_{P,i} (\hat{X}_{i,k+1}^{\text{f}} - x_{k+1}^{\text{f}})(\hat{X}_{i,k+1}^{\text{f}} - x_{k+1}^{\text{f}})^T + Q_k, \quad (6.12)$$

$$X_{k+1}^{\text{f}} = \Psi(x_{k+1}^{\text{f}}, P_{k+1}^{\text{f}}, \lambda). \quad (6.13)$$

Since UKF involves  $2n + 1$  model update, the computational burden of UKF is of the order  $(2n + 1)n^2 = 2n^3 + n^2$ . On the other hand, XKF involves a single model update and covariance propagation using the Riccati equation and hence the computational burden of XKF is of the order  $n^3 + n^2$ . Hence, when  $n$  is large the computational burden of UKF is approximately twice that of XKF. The performance of UKF and XKF are compared in [10].

## VII. THE UNSCENTED $H_\infty$ FILTER

Finally, we consider an extension of UKF that is based on the  $H_\infty$  filter. The analysis step of the unscented  $H_\infty$  filter (UHF) is given by (6.2)-(6.4) with

$$P_k^{\text{da}} = \tilde{P}_k^{\text{f}} - K_k \tilde{P}_{yy,k} K_k^T, \quad (7.1)$$

where

$$K_k = \tilde{P}_{xy,k} \tilde{P}_{yy,k}^{-1}, \quad (7.2)$$

$$\tilde{P}_{xy,k} = \sum_{i=0}^{2n} \gamma_{P,i} (\tilde{X}_{i,k}^{\text{f}} - x_k^{\text{f}})(\tilde{Y}_{i,k}^{\text{f}} - y_k^{\text{f}})^T, \quad (7.3)$$

$$\tilde{P}_{yy,k} = \sum_{i=0}^{2n} \gamma_{P,i} (\tilde{Y}_{i,k}^{\text{f}} - y_k^{\text{f}})(\tilde{Y}_{i,k}^{\text{f}} - y_k^{\text{f}})^T + R_k, \quad (7.4)$$

$$\tilde{Y}_{i,k}^{\text{f}} = h(\tilde{X}_{i,k}^{\text{f}}, k), \quad (7.5)$$

and the forecast step of UHF is given by (6.10)-(6.12),  $\tilde{X}^{\text{f},k}$  is obtained using

$$\tilde{X}_{k+1}^{\text{f}} = \Psi(x_{k+1}^{\text{f}}, \tilde{P}_{k+1}^{\text{f}}, \lambda), \quad (7.6)$$

and  $\tilde{P}_k^{\text{f}}$  is defined by (3.7).

Note that when the dynamics are linear, then UHF is equivalent to XHF presented in Section 3.

## VIII. EXAMPLES

Next, we use XKF, XHF, UKF, and UHF for state estimation of low-dimensional discrete-time systems with nondifferentiable nonlinearities. Specifically, we consider nonlinearities that are not differentiable but have symmetric derivatives everywhere.

### A. Absolute Value Function

First, we consider nonlinearities that commonly occur in finite volume discretization of hyperbolic partial differential equations [13]. For example, the absolute value function appears in the first-order upwind discretization of an advection equation [13]. Let  $x \in \mathbb{R}^4$  and

$$x_{k+1} = \text{abs}(\sin(Mx_k)) + w_k, \quad (8.1)$$

$$y_k = Cx_k + v_k,$$

where  $M \in \mathbb{R}^{4 \times 4}$  and

$$C = \begin{bmatrix} 1 & 0 & 0 & 0 \\ 0 & 0 & 0 & 1 \end{bmatrix}, \quad (8.2)$$

and  $w_k$  and  $v_k$  are zero-mean white processes with covariances  $Q_k = 0.1I_4$  and  $R_k = 0.01I_2$ , respectively. Note that for all  $x \in \mathbb{R}$ ,

$$\frac{\partial_s \text{abs}(\xi)}{\partial_s \xi} \Big|_{\xi=x} = \begin{cases} 1, & \text{if } x > 0, \\ -1, & \text{if } x < 0, \\ 0, & \text{if } x = 0. \end{cases} \quad (8.3)$$

Hence, it follows from (4.9), (8.1) and (8.3) that for  $i, j = 1, \dots, n$ , the  $(i, j)$  entry of  $F_s(x)$  is given by

$$F_{s,i,j}(x) = \begin{cases} \cos(\text{row}_i(M)x)M_{i,j}, & \text{if } \sin(\text{row}_i(M)x) > 0, \\ -\cos(\text{row}_i(M)x)M_{i,j}, & \text{if } \sin(\text{row}_i(M)x) < 0, \\ 0_{1 \times 4}, & \text{if } \sin(\text{row}_i(M)x) = 0, \end{cases} \quad (8.4)$$

where  $\text{row}_i(M)$  is the  $i$ th row of  $M$ , and  $H_s(x) = C$ .

Figure 1 shows a plot of  $\text{abs}(\sin(mx))$  and it can be seen that as  $m$  increases, the nonlinearities become more prominent. The logarithm of the sum of the Euclidean norms of the errors in the state estimates for 50 different choices of  $M$  with  $\text{sprad}(M) = 0.5$  is shown in Figure 2. Numerical simulations suggest that the performance of XKF, XHF, UKF, and UHF is almost indistinguishable for all choices of  $M$ . The error in the state estimates when no data assimilation is performed, that is,  $K_k = 0$  for  $k \geq 0$  in XKF, is also plotted for comparison. Next, the performance of all the estimators for 50 different choices of  $M$  with  $\text{sprad}(M) = 10$  is shown in Figure 3. It can be seen that in the case of more severe nonlinearities, the performance of UKF and UHF is better than the performance of XKF and XHF. The values of  $\gamma$  in all the cases were chosen such that XHF and UHF are both stable.

### B. Minmod Function

Next, we consider discrete-time systems involving the minmod function, which is used in second-order upwind finite volume schemes as a slope limiter to reduce the diffusion effects [13]. For  $\alpha, \beta \in \mathbb{R}$ , define

$$\text{minmod}(\alpha, \beta) = \frac{1}{2} (\text{sign}(\beta) + \text{sign}(\alpha)) \min\{|\alpha|, |\beta|\} \quad (8.5)$$

(see Figure 4). Let  $x \in \mathbb{R}^{10}$  and

$$\begin{aligned} x_{k+1} &= \sin(Mx_k) + \text{minmod}(M_L x_k, M_R x_k) + w_k, \\ y_k &= Cx_k + v_k. \end{aligned} \quad (8.6)$$

We choose  $M \in \mathbb{R}^{10 \times 10}$  so that  $\text{sprad}(M) < 1$ , and for  $i, j = 1, \dots, 10$ , the  $(i, j)$  entry of  $M_L \in \mathbb{R}^{10 \times 10}$  is given by

$$(M_L)_{i,i} = 1, \quad (M_L)_{i,i-1} = -1, \quad (M_L)_{i,j} = 0 \text{ if } j \notin \{i, i-1\}, \quad (8.7)$$

$M_R = -M_L^T$ , and for all  $k$ ,  $C_k \in \mathbb{R}^{2 \times 10}$  is chosen to be

$$C_k = \begin{bmatrix} 1 & 0_{1 \times 9} \\ 0_{1 \times 9} & 1 \end{bmatrix}. \quad (8.8)$$

We assume that  $w_k$  and  $v_k$  are zero-mean white processes with covariances  $Q_k = 0.1I_{10}$  and  $R_k = 0.01I_2$ , respectively. Note that for all  $u, v \in \mathbb{R}$ ,

$$\frac{\partial_s}{\partial_s \alpha} \text{minmod}(\alpha, \beta) \Big|_{(u,v)} = \begin{cases} 0, & \text{if } uv < 0 \text{ or } u = v = 0, \\ 0, & \text{if } uv > 0 \text{ and } |u| > |v|, \\ 0, & \text{if } u \neq 0, v = 0, \\ 0.5, & \text{if } uv > 0 \text{ and } |u| = |v|, \\ 0.5, & \text{if } u = 0, v \neq 0, \\ 1, & \text{if } uv > 0 \text{ and } |u| < |v|. \end{cases} \quad (8.9)$$

Furthermore, (8.6) implies that  $H_s(x) = C$ .

The sum of the Euclidean norm of the error in the state estimates obtained from XKF, XHF, UKF, and UHF for 50 different choices of  $M$  with  $\text{sprad}(M) = 0.5$ , is shown in Figure 5. The performance of the four estimators for 50 different choices of  $M$  with  $\text{sprad}(M) = 10.0$  is shown in Figure 6.

## IX. SIMULATION EXAMPLE : ONE-DIMENSIONAL HYDRODYNAMICS

Finally, we consider state estimation of one-dimensional hydrodynamic flow based on a finite volume model. The flow of an inviscid, compressible fluid along a one-dimensional channel is governed by Euler's equations. A discrete-time model of hydrodynamic flow can be obtained by using a finite-volume based spatial and temporal discretization.

Assume that the channel consists of  $n$  identical cells. For all  $i = 1 \dots n$ , define  $U^{[i]} \in \mathbb{R}^3$  by  $U^{[i]} = [\rho^{[i]} \quad m^{[i]} \quad \mathcal{E}^{[i]}]^T$ , where  $\rho^{[i]}$  is the density,  $m^{[i]}$  is the momentum and  $\mathcal{E}^{[i]}$  is the energy in the  $i$ th cell. We use a second-order Rusanov scheme [13] to discretize Euler's equations and obtain a discrete-time model that enables us to update the flow variables at the center of each cell. Define the state vector  $x \in \mathbb{R}^{3(n-4)}$  by

$$x \triangleq \left[ (U_k^{[3]})^T \quad \dots \quad (U_k^{[n-2]})^T \right]^T. \quad (9.1)$$

For all  $k \geq 0$ , let  $u_k \in \mathbb{R}^3$  denote the boundary condition for the first two cells, so that  $u_k = (U_k^{[1]})^T = (U_k^{[2]})^T$ . Furthermore, we assume Neumann boundary conditions at cells with indices  $n-1$  and  $n$ . The second-order Rusanov scheme yields a nonlinear discrete-time update model of the form (4.1), where  $w_k \in \mathbb{R}^{3(n-4)}$  represents unmodeled drivers and is assumed to be zero-mean white Gaussian process noise with covariance matrix  $Q \in \mathbb{R}^{3(n-4) \times 3(n-4)}$  such that only the flow variables in the 10th, 25th and 40th cell are directly affected by  $w_k$ . We assume that measurement  $y_k \in \mathbb{R}^6$  of density, momentum and energy at cells with indices 6, 16, 26, 35, and 42 are available and  $v_k$  is zero-mean white Gaussian noise with covariance matrix  $R = 0.01I_{15 \times 15}$ . Let  $n = 54$  so that  $x \in \mathbb{R}^{150}$ . For all  $k \geq 0$ , let  $\rho_k^{[1]} = \rho_k^{[2]} = 1 \text{ kg/m}^3$ ,  $m_k^{[1]} = m_k^{[2]} = v_{\text{in}} + \frac{v_{\text{in}}}{4} \sin(k)$  m/s, and  $SE_k^{[1]} = \mathcal{E}_k^{[2]} = (1/2)(m_k^{[1]})^2/\rho_k^{[1]} + 3/2 \text{ N/m}^2$ , where  $v_{\text{in}}$  is the inlet velocity.

We simulate the truth model from an arbitrary initial condition  $x_0 \in \mathbb{R}^{3(n-4)}$  and obtain measurements  $y_k$  for various choices of  $v_{\text{in}} \in \{0.0, 1.0, 2.0, \dots, 10.0\}$  m/s. Note that if  $v_{\text{in}} > 1.29$  m/s, then the flow is supersonic. The objective is to estimate the density, momentum, and energy at the cells where measurements of flow variables are unavailable using XKF and UKF. It follows from (3.7) that XHF and UHF involve inverting a  $n \times n$  matrix which is computationally intensive when  $n$  is large which is the case in finite volume discretization of partial differential equations. Moreover, in the previous examples, no significant improvement in performance was noticed when the XHF and UHF were used instead of XKF and UKF, respectively. Hence, we do not use XHF or UHF for state estimation in the one-dimensional hydrodynamic flow example.

The error in the estimates of the energy  $\mathcal{E}_k^{[30]}$  in cell 30, when measurements  $y_k$  are used in XKF and UKF with  $v_{\text{in}} = 1$  m/s is shown in Figure 7. The error in estimates of the energy  $\mathcal{E}_k^{[30]}$  in cell 30, when  $v_{\text{in}} = 10$  m/s is shown in Figure 8. The sum of the Euclidean norm of error in the state

estimates for different values of  $v_{in}$  is shown in Figure 9. Note that at low inlet velocities  $v_{in}$ , the performance of XKF and UKF is very similar. However, at higher inlet velocities, the nonlinearities are more severe and the performance of UKF is better than that of XKF.

## X. CONCLUSION

In this paper we compared the performance of the extended Kalman filter, the extended  $H_\infty$  filter, the unscented Kalman filter, and the unscented  $H_\infty$  filter for nonlinear systems with nondifferentiable nonlinearities. Whenever the Jacobian fails to exist, we use an averaged Jacobian based on the symmetric derivatives in the extended Kalman filter. For all the examples that we considered, whenever the nonlinearities are not severe, the performance of XKF with the averaged Jacobian and UKF is similar. However, when the nonlinearities become severe, UKF performs better than XKF. No significant improvement in the performance was noticed when either the extended  $H_\infty$  filter or the unscented  $H_\infty$  filter was used over the extended Kalman filter and unscented Kalman filter, respectively.

## REFERENCES

- [1] M. Athans, R. P. Wishner, and A. Bertolini, "Suboptimal State Estimation for Continuous-Time Nonlinear Systems from Discrete Noisy Measurements," *IEEE Trans. Auto. Ctrl.*, vol. 13, pp. 504–514, 1968.
- [2] K. Ito and K. Xiong, "Gaussian Filters for Nonlinear Filtering Problems," *IEEE Trans. Auto. Ctrl.*, vol. 45, pp. 910–927, 2000.
- [3] J. M. Lewis, S. Lakshminarayanan, and S. Dhall, *Dynamic Data Assimilation: A Least Squares Approach*. Cambridge University Press, 2006.
- [4] A. Jazwinski, *Stochastic Processes and Filtering Theory*. Academic Press, 1970.
- [5] A. Gelb, *Applied Optimal Estimation*. Cambridge: MIT Press, 1974.
- [6] J. Chandrasekar, A. J. Ridley, and D. S. Bernstein, "A SDRE-Based Asymptotic Observer for Nonlinear Discrete-Time Systems," in *Proc. Amer. Contr. Conf.*, Portland, OR, June 2005, pp. 3630 – 3635.
- [7] C. P. Mracek, J. R. Cloutier, and C. A. D'Souza, "A New Technique for Nonlinear Estimation," in *Proc. Int. Conf. Contr. App.*, Dearborn, MI, June 1996, pp. 338–343.
- [8] W. Sun, K. M. Nagpal, and P. P. Khargonekar, " $H_\infty$  Control and Filtering for Sampled-Data Systems," *IEEE Trans. Auto. Ctrl.*, vol. 38, pp. 1162–1175, 1993.
- [9] E. G. Collins Jr. and T. Song, "Robust  $H_\infty$  Estimation and Fault Detection of Uncertain Dynamic Systems," *Int. J. Guid. Cont. Dyn.*, vol. 23, no. 5, pp. 857–864, 2000.
- [10] S. Julier, J. Uhlmann, and H. F. Durrant-Whyte, "A New Method for the Nonlinear Transformation of Means and Covariances in Filters and Estimators," *IEEE Trans. Auto. Ctrl.*, vol. 45, pp. 477–482, 2000.
- [11] R. V. der Merwe and E. A. Wan, "The Square-root Unscented Kalman Filter for State and Parameter Estimation," in *Proc. Int. Conf. Acou. Speech Sig. Process.*, May 2001, pp. 3461 – 3464.
- [12] C. Groth, D. D. Zeeuw, T. Gombosi, and K. Powell, "Global 3D MHD Simulation of a Space Weather Event: CME Formation, Interplanetary Propagation, and Interaction with the Magnetosphere," *J. Geophys. Res.*, vol. 105, pp. 25 053–25 078, 2000.
- [13] C. Hirsch, *Numerical Computation of Internal and External Flows*. John Wiley and Sons, 1990.
- [14] B. D. O. Anderson and J. B. Moore, *Optimal Filtering*, Dover Publications Inc., Mineola, NY, 1979.
- [15] L. Scherliess, R. W. Schunk, J. J. Sojka, and D. C. Thompson, "Development of a Physics-based Reduced State Kalman filter for the Ionosphere," *Radio Science*, vol. 39, 2004.
- [16] L. Larson, "The Symmetric Derivative," *Trans. Amer. Math. Soc.*, vol. 277, pp. 589–599, 1983.

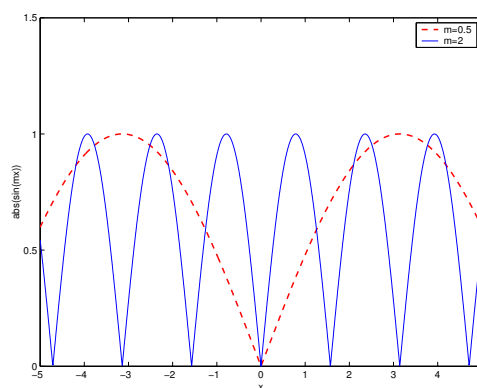


Fig. 1. Plot of  $\text{abs}(\sin(mx))$  for  $m = 0.5$  and  $m = 2$ .

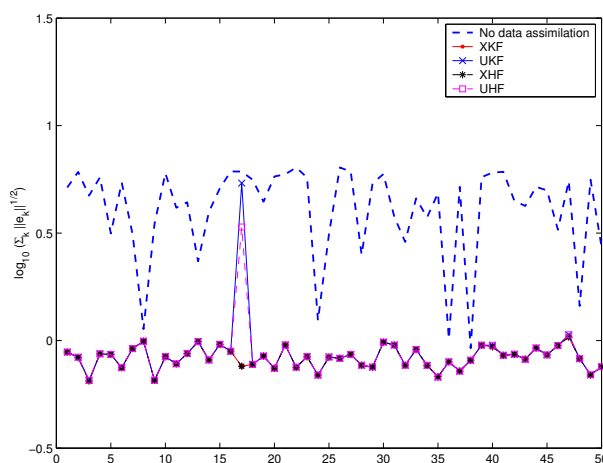


Fig. 2. Logarithm of the sum of Euclidean norms of the errors in state estimates obtained using XKF, XHF, UKF, and UHF for the system (8.1). The performance is compared for 50 different choices of  $M$  with  $\text{sprad}(M) = 0.5$ . The error in the estimates when no data assimilation is performed, that is,  $K_k = 0$  for all  $k \geq 0$  in XKF is also shown for comparison.

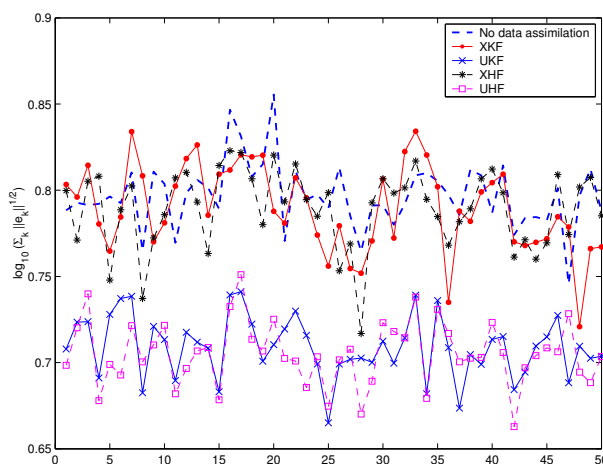


Fig. 3. Logarithm of the sum of the Euclidean norms of the errors in state estimates obtained using XKF, XHF, UKF, and UHF for the system (8.1). The performance is compared for 50 different choices of  $M$  with  $\text{sprad}(M) = 10$ . The performance of UKF and UHF is much better than the performance of XKF or XHF. However, the performances of XKF and UKF are very similar to the performance of XHF and UHF, respectively.

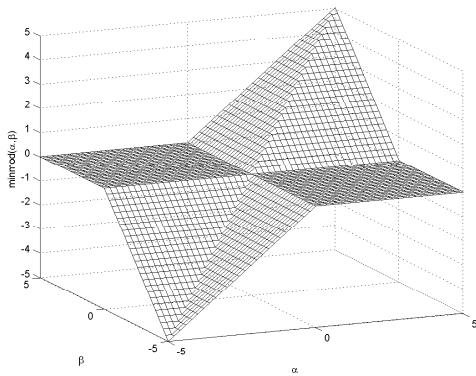


Fig. 4. Plot of  $\min\text{mod}(\alpha, \beta)$  for  $-5 \leq \alpha, \beta < 5$ .

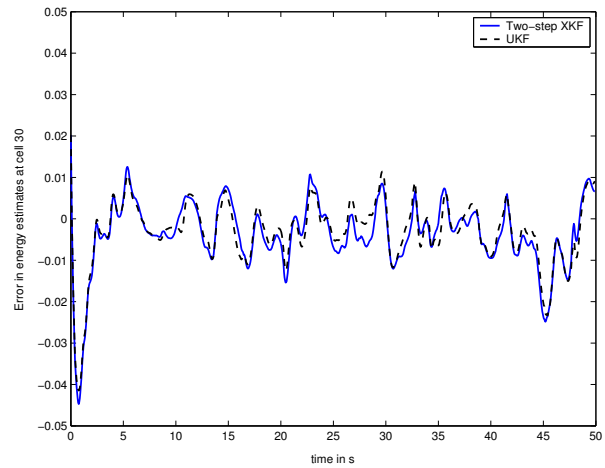


Fig. 7. The error in the estimates of energy at cell 30 obtained using XKF and UKF when  $v_{in} = 1$  m/s and the flow is subsonic.

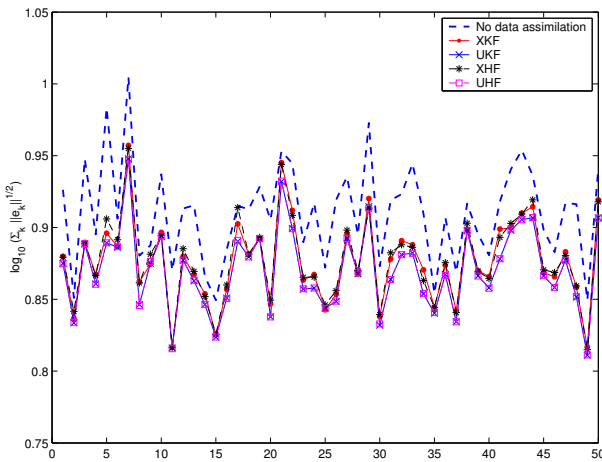


Fig. 5. Logarithm of the sum of the Euclidean norms of the errors in state estimates obtained using XKF, XHF, UKF, and UHF for the system (8.6). The performance of the four estimators are compared for different choices of  $M$  with  $\text{sprad}(M) = 0.5$ . We choose the largest possible  $\gamma (=1.5)$  such that both XHF and UHF are stable for all choices of  $M$ .

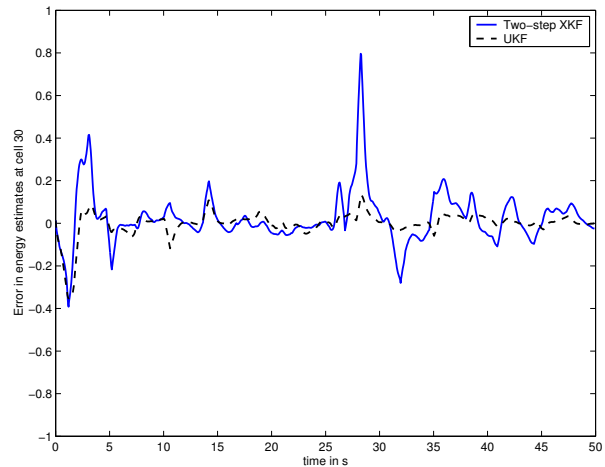


Fig. 8. The error in the estimates of velocity at cell 30 obtained using XKF and UKF when  $v_{in} = 10$  m/s and the flow is supersonic with Mach number 7.75.

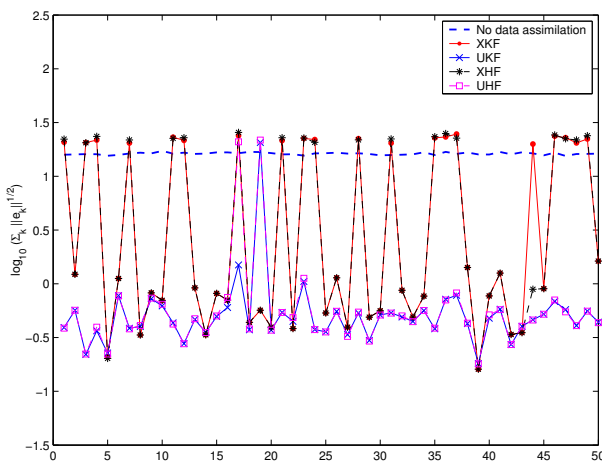


Fig. 6. Logarithm of the sum of the Euclidean norms of the errors in state estimates obtained using XKF, XHF, UKF, and UHF for the system (8.6). The performance of the two estimators is compared for 50 different choices of  $M$  with  $\text{sprad}(M) = 10.0$ . There seems to be no significant improvement in the performance when the  $H_\infty$  filters (XHF and UHF) are used over XKF and UKF, respectively.

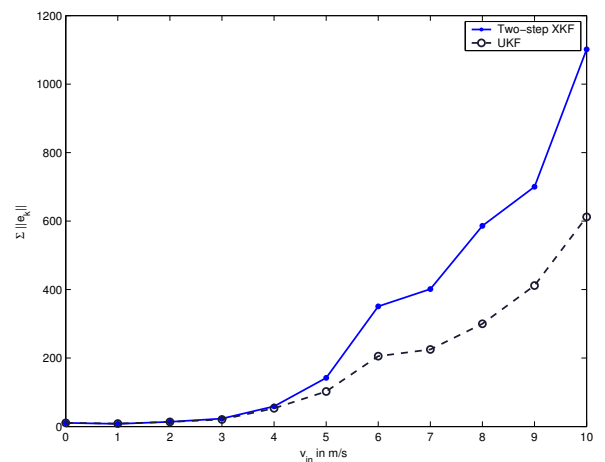


Fig. 9. The square root of the sum of the Euclidean norms of the errors in state estimates, obtained using XKF and UKF for different choices of the inlet velocity  $v_{in}$ . The performance of UKF is better than the performance of XKF for high inlet velocities, with a computational burden that is twice that of XKF.